

# EXPERIMENTAL AND NUMERICAL ANALYSIS ON FRICTION STIR WELDING OF HIGH STRENGTH METALS AT PLUNGE STAGE

Vuppula Prasanna<sup>a</sup> & Dr. P. Ramesh Babu<sup>b</sup>

<sup>a</sup>Assistant Professor, Institute of Aeronautical Engineering, Dundigal, Hyderabad-500043, India.

<sup>b</sup> Professor & Head of Mechanical Department, Osmania University, Hyderabad-500007, India.

aorcid id: 0000-0003-0860-8742

## Abstract

A Numerical simulation at plunge stage model was developed to study the temperature fields and the plastic deformations of Al alloy 6061-T6 and Mg alloy AE42 under different rotating speeds: 800,1200 rpm and travel speeds : 60mm/min ,50 mm/min with constant axial load of 40 KN during the friction stir welding (FSW) process. Observations by optical microscopy shows weld geometry of the weldments. Coarse grains are found to be in the HAZ and finest grains were observed within the nugget. Three dimensional finite element model has been developed in ABAQUS/EXPLICIT using the arbitrary Lagrangian-Eulerian formulation, the Johnson-Cook (JC) elastic-plastic model and Coulomb's Law of friction is used. The JC model defines the strength of the material as a function of three parameters i.e. the strength of the material depends on the strain hardening effects, strain rate effects and temperature. Results indicate the maximum temperature by numerical analysis. If rotational speed, travel speed increases the plunge force will be reduced in friction stir welding process.

**Keywords:**FSW, Process parameters, mechanical test, metallography, numerical simulation, plunge stage, temperature, force

## 1. INTRODUCTION

Welding technology plays a key role in structure's manufacturing by reducing cost in joining materials [1]. To achieve the goal Friction stir welding (FSW) was introduced[2].

FSW has become the most effective technology in solving problems that have reached the profiled sheets with the continuation of material, particularly in the aerospace industry, with the use of different joining techniques that require high ductility and tensile strength. Current study, FS weldments AA6061-T6 to AE42 magnesium alloy were successfully obtained with varying processing parameters and were mechanically and metallurgically characterized [3, 4]. This paper discuss on macrostructure analysis, influence of tool geometry, process parameters with numerical study.

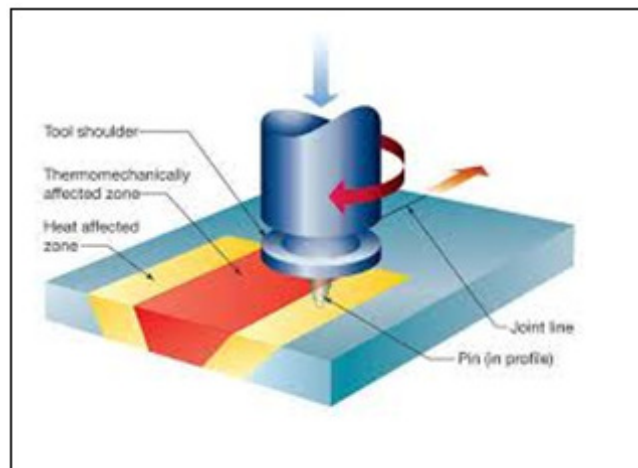


Figure 1. Schematic Illustration of FSW Process

## 2. EXPERIMENTAL SETUP

## 2.1 Material and Specimen preparations

Welding plate sizes are 120mm x 100 mm x 3mm were used. Cast AA6061-T6, belongs to aluminium alloys. Copper and magnesium grows at its peak and elevated temperatures when its strength and hardness grows. Dissimilar metals properties and compositions are given in below tables. It has good weldability and corrosion resistance. The sides of the plates will be checked for parallel to the correct clamp in the FSW divisions, which will consolidate the movement for the welding process of movement.

TABLE 2. Mechanical properties of Aluminium Base metal AA6061-T6 alloy

Alloy AA6061-T6	0.2% Yield Strength (MPa)	UTS (MPa)	Elongation (%)	Hardness (VHN)
Standard	198	240	26	105
Observed	183	236	22	103

TABLE 3. Chemical Composition of the base metals (Wt. %) of Magnesium AE42 alloy

Wt. %	Al	Zn	RE(Ce+ Nd+ La+ Th+ Pr)	Mn	Mg
Standard	4	-	2(1.2+0.4+0.6+0.1+0.1)	0.3	Balance
Observed	3.9	0.08	2.2	0.31	Balance

TABLE 4. Mechanical properties of Magnesium Base Metal AE42 alloy

Alloy AE42	Yield Strength (MPa)	UTS (MPa)	Elongation (%)	Hardness (VHN)
Standard	130	225	6	75
Observed	124	198	3	72

TABLE 5. Mechanical Characteristics of parent material Al alloy 6061-T6 and Mg alloy AE42

Material Properties	Value of Al 6061-T6	Value of Mg AE42
Young's Modulus of Elastic (Gpa)	198	120
Poisson's ratio	0.33	0.35
Thermal Conductivity (W/m-K)	167	139
Coefficient of Thermal Expansion (°C <sup>-1</sup> )	23.4x10 <sup>-6</sup>	26.1x10 <sup>-6</sup>
Density (kg/m <sup>3</sup> )	2.7	1.80
Specific Heat Capacity J/(Kg °C)	0.896	1.45
Latent Heat (J/g)	400	373
Temperature of melt (°C)	412	435

## 2.2 FS welding Tool Design

Tool shoulder diameter, D (mm) : 12

Tool shoulder length, L (mm) : 16

Pin diameter, d (mm) : 2.5

D/d ratio of tool : 4.8

Pin length, L (mm) : 2.9

Pitch (mm) of threaded pin : 1

FSW depends on design of tool, process parameters. Design of tool and geometry of it's made. For current research on aluminium alloy AA6061-T6 and magnesium alloy AE42 a conical tapered threaded pin profile has been used for high speed steel material with 60HRC hardness.

TABLE 6. Parameters of Dissimilar Weldments

S. No	Rotational Speed (rpm)	Travel speed (mm/min)	Width (mm)	Thickness (mm)	Sp. Gauge length (mm)	0.2 Yield Strength (MPa)	Ultimate Tensile Strength (MPa)	Elongation (%)	Efficiency ( $\eta$ ) %
1	800	150	5	3	25	140	190	3.0	84.4
2	1200	150	5	3	25	165	187	3.5	83.1
3	800	60	5	3	25	124	167	3.0	74.2
4	1200	60	5	3	25	123	155	3.0	68.8

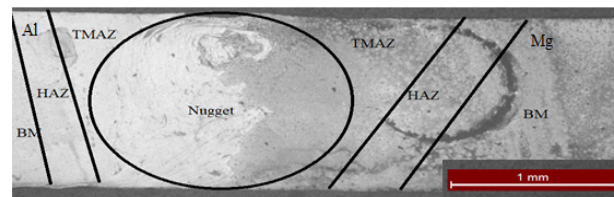
From table 6, shows the samples process parameters and their joint efficiencies are high at 800 rpm with 150 mm/min travel speed and minimum at 1200 rpm with 60 mm/min travel speed. To find out the cause of deviation in the tensile specimens, macrostructure analysis, microstructure analysis and micro hardness measurements are performed



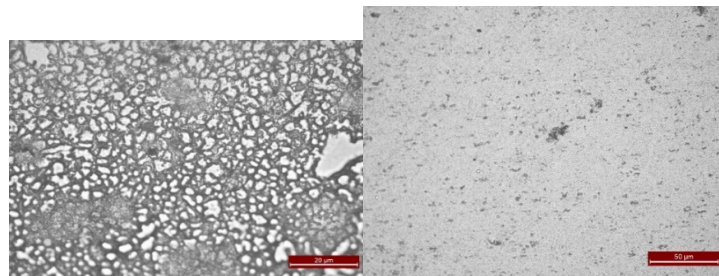
**Figure 2.**The fracture location of the tensile specimens' joints welded at rotation speed of 800 rpm and 1200rpm

### 2.3 Microstructure Evaluation

Macro and Microstructure shown in fig (3, 4) at cross-section. The heat affected zone (HAZ) has changes in mechanical properties, revised at the region thermo-mechanically affected zone (TMAZ) in which the material was deformed plastically. Centre line termed as stirred zone with fine, equivalent refined grains.



**Figure 3.**Macrostructure of a FSW joint



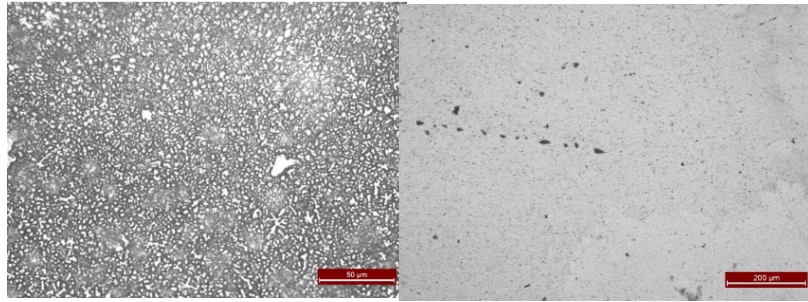


**Figure 4.**Microstructure of Weldments at nugget zone

## 2.4 Microhardness

Vickers microhardness of weldments are measured with the dotted lines shown in fig 5. Fig 5 shows an uneven distribution. An average hardness values of dissimilar metals are given in table 2 and 4. At NZ values depend on the range of phase constituents and local recrystallization. Maximum hardness (HV) shown at the cross section at nugget zone, but the hardness value is not much higher than the base material [6]. Then, microhardness base material is less than the value of the AA6061-T6 and slowly increases at one side, another side Mg AE42 is at the medium level.

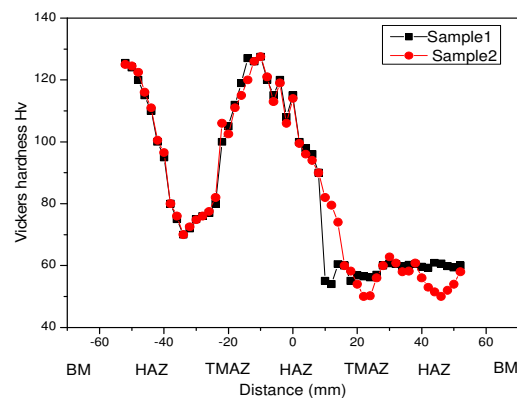


**Figure5.**Vickers hardness graph

## 3. MODEL DESCRIPTIONS

The basic model is composed of a coupled thermo mechanical finite element model developed in abaqus/explicit including mesh formulation, the Johnson cook (JC) material model and coulomb's law of friction is used [10-14].

### 3.1 Geometry, boundary conditions and the FE mesh

3-D numerical model is based on the C3D8RT element type, which is a thermo mechanically coupled hexahedral element with 8 nodes, each having trilinear displacement. Plate dimensions in the numerical model at the plunge stage is 120mmx100mmx3mm. The mesh consists of 23608 nodes and 20972 elements. The numerical model of the welding plate, tool is shown in the figure 6.

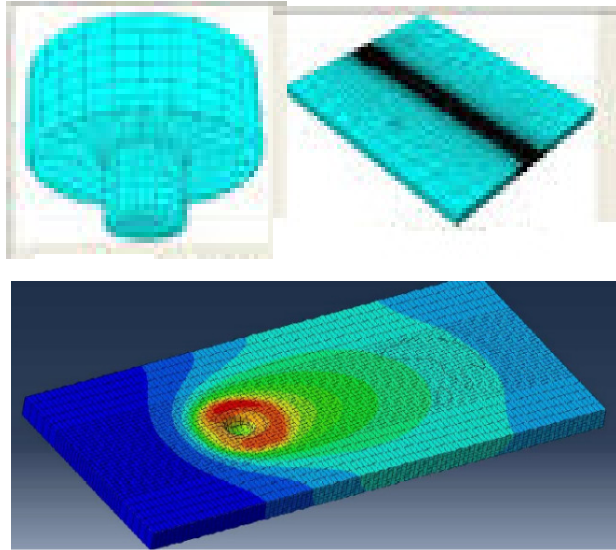


**Figure 6.** Numerical model of the welding plate, and the tool

### 3.2 Thermal model

FSW heat generation sources: frictional heating at the tool work piece interface and plastic energy dissipation due to shear deformation in the nugget zone [15-21]. When heat is dissipated by conduction into the workpiece, tool and backing plate, and also by convection and radiation from the surfaces. Traditional losses are considered in this model are lower because of lower temperatures. They can be combined with convection from the top surface of the plate by using a slightly higher heat transfer coefficient, the governing equation for heat transfer is

$$\frac{\partial}{\partial x} \left( k \frac{\partial T}{\partial x} \right) + \frac{\partial}{\partial y} \left( k \frac{\partial T}{\partial y} \right) + \frac{\partial}{\partial z} \left( k \frac{\partial T}{\partial z} \right) + q_v = \rho c_p \frac{\partial T}{\partial t}$$

Where

$k$  is the materials conductivity W/mK

$q_v$  is the rate at which energy is generated per unit volume of the medium W/m<sup>3</sup>

$\rho$  is the density kg/m<sup>3</sup>

$c_p$  is the specific heat capacity J/ (Kg °C)

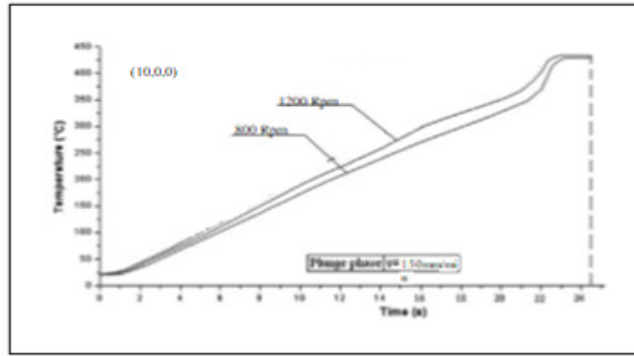


Figure 7. Temperature dependence of the time at point T during the plunge stage

### 3.3 Johnson-cook elastic-plastic model

This process results in a large deformation in the thermomechanically affected zone. Modelling the FSW process requires the interaction of flow pressure with temperature, plastic strain, and strain rate. For this reason the Johnson-Cook elastic-plastic model has been implemented [22-25]. The formulation for this model is empirically based. The Johnson-cook elastic-plastic model equation is given by

$$\sigma_{JC} = [A + B\varepsilon^n][1 + C \ln \frac{\dot{\varepsilon}}{\dot{\varepsilon}_0}][1 - (\frac{T - T_r}{T_m - T_r})^m]$$

TABLE 7. Johnson cook elastic plastic constants for dissimilar metals

Dissimilar Metals	A	B	n	m	Melting temp $T_m(^{\circ}C)$	Ambient temp $T_r(^{\circ}C)$
AA6061-T6	285	94	0.41	1.34	588	25
Mg AE42	172	360.7	0.45	0.95	650	25

A, B, n,  $T_m$ ,  $T_r$  and m are the material constants for Johnson Cook strain rate dependent yield stress for dissimilar metals as shown in table 7, where  $T_m$  = the melting point or the solidus temperature,  $T_r$  = ambient temperature, A = yield stress, B = strain factor, n = strain exponent, m = temperature exponent.

### 4. RESULTS AND DISCUSSIONS

The analysis of experimental weldments of Al alloy 6061-T6 to Magnesium alloy AE42 shows the maximum hardness at the weld joint compared to the parent material.

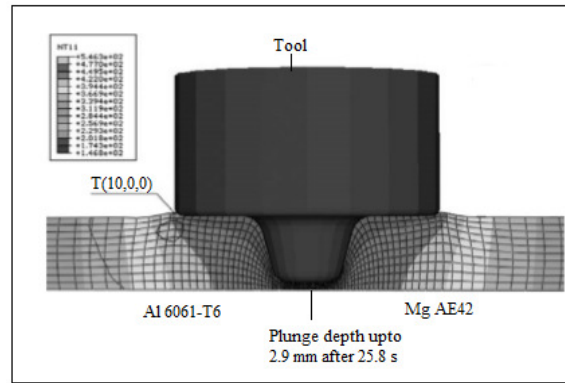


**Figure 8.** Temperature fields in the transverse cross-section near tool interface after 25.8 s, when rotation speed at 1200 rpm and plunge speed at 60mm/min.

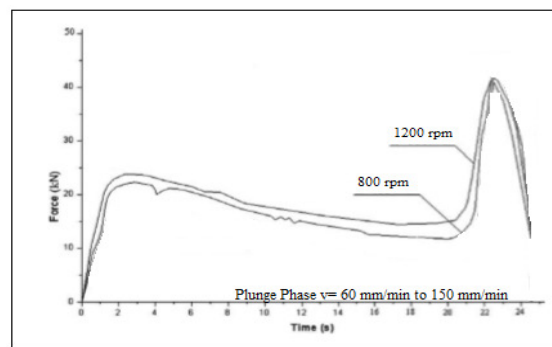


**Figure 9.** Force dependence of the time during the plunge stage

Study of temperature fields and the plunge force of Al alloy 6061-T6 to magnesium alloy AE42 was developed by coupled thermomechanical model, under different rotating speeds: (800, 1200) rpm with travel speeds of 150mm/min and 60mm/min. Figure 8 shows the coordinates of point T (10, 0, 0) used for measuring the temperature dependence of the time.

The heat transfer coefficient through the welding plate is  $687 \text{ W/m}^2 \text{ K}$ , A constant coefficient of friction is 0.3 assumed between the tool and the welding with corresponding heat convective coefficients on the surface of the welding plates are  $h=10 \text{ W/m}^2\text{K}$  with the ambient temperature of  $200 \text{ }^\circ\text{C}$  at 25.8 s. when the plunge speed is 15mm/min and the rotation speed is 600mm/min.

#### 4. CONCLUSION

Observations of macrostructure and microstructure shows different zones of weldments. Coarse grains were found to be in HAZ and fine grains within the nugget. Tensile strength of the parent material found was 84%. This behavior is related to the plastic deformation effect of heat generated by surface friction plastic deformation.

The highest temperature produced by weldments can range from 85% - 95% to the melting temperature of the base material. As the speed of rotation increases, the area of temperature increases. The temperature field is symmetrical. The contact between the rotating pin and the welding plate begins to increase, and reaches a maximum value at 1200 rpm and 800 rpm due to the material plasticity and is softened due to high pressure and

temperature rise. As the speed of rotation increases, the plunge force can be reduced. The results show that software ABAQUS is particularly important in simulating mechanical properties in this process.

## 5. ACKNOWLEDGEMENT

The author gratefully acknowledge DMRL, Hyderabad for providing young researchers to do their project work for few months. I thank each technician who ever have helped me in this project in R&D laboratory for taking Microstructures and testing Mechanical Properties on metals.

## 6. REFERENCES

- [1] S. W. Kallee. Friction Stir Welding - How to weld aluminium without melting it, Innovation for new rail business IMechE, London, 2001 [www.twi.co.uk/j32k/protected](http://www.twi.co.uk/j32k/protected).
- [2] W. M. Thomas and E. D. Nicholas, Friction stir welding for the transportation industries, Materials & Design, vol. 18, pp. 269-273, 1997.
- [3] W. M. Thomas, E. D. Nicholas, J. C. Needham, M. G. Nurch, P. Temple-Smith, and C. Dawes, Patents on Friction Stir Butt Welding, International: PCT/GB92/02203; British: 9125978.8; USA: 5460317. 1991-1995.
- [4] Troeger L. P. Starke E. A., Microstructural and mechanical characterization of a Superplastic 6xxx aluminium alloy, Materials Science and Engineering, A277, pp. 102-113, 2000.
- [5] Matrukanitz R.P. (1990), 'Selection and weldability of heat-treatable aluminium alloys, ASM handbook- Welding, Brazing and Soldering, Vol.6, pp. 528-536.
- [6] Rhodes C.G., Mahoney M.W. and Bingel W.H. (1997), 'Effect of friction stir welding on microstructure of 7075 aluminium', Scripta Materilaia, Vol. 36, N0\o. 1, pp.69-75.
- [7] Su J.Q., Nelson T.W., Mishra R. and Mahoney M. (2003), 'Microstructural investigation of friction stir welded 7050-T651 aluminium', Acta Materilaia, Vol. 51, No. 3, pp. 713-729.
- [8] Arora, H.S., Singh, H., and Dhindaw, B.K., (2011), Parametric Study of Friction Stir Processing of Magnesium-Based AE42 Alloy, Journal of Materials Engineering and Performance, 21(11), 2328-2330.
- [9] Gregg P, Proceedings of the 6th International Conference Magnesium Alloys and Their Applications, Ed. K.U. Kainer, Wiley-VCH, (2003), PP.524-528

- [10] Z. Zhang, J. Bie, H. Zhang, Effect of Traverse/Rotational Speed on Material Deformations and Temperature Distributions in Friction Stir Welding, *J. Mater. Sci. Technol.*, 24 (2008), 907–913
- [11] H. Schmidt, J. Hattel, A local model for the thermo-mechanical conditions in friction stir welding, modelling *Simul. Mater. Sci. Eng.*, 13 (2005), 77–93 10 Abaqus Inc., Analysis User's Manual v.6.7, 2007
- [12] D. Veljic, M. Perovic, B. Medjo, M. Rakin, A. Sedmak, H. Dascau, Thermo-mechanical modeling of Friction Stir Welding, the 4th International Conference, Innovative technologies for joining advanced materials, Timisoara, 2010, 171–176 12
- [13] V. Prasanna, Dr. A. Seshu Kumar, Dr. P. Ramesh Babu, “Friction Stir Welding of Magnesium Alloys- A Review” *International Journal of Advanced Engineering Research and Science*, Vol-3, Issue-12, Dec-2016.
- [14] V. Prasanna, Dr. A. Seshu Kumar, Dr. P. Ramesh Babu, “Analogy of Conventional Welding Methods with Solid-State Welding Techniques” *Imperial Journal of Interdisciplinary Research*, Vol-2, Issue-9, 2016.
- [15] H. Dascau, A. Sedmak, M. Rakin, D. Veljic, M. Perovic, B. Medjo, N. Bajic, Numerical simulation of the plunge stage in friction stir welding – different tools, The 5th International Conference, Innovative Technologies for joining advanced materials, Timisoara, 15, 2011, 1–4
- [16] Reynolds, A., Friction Stir Welding of Aluminium Alloys, in: *Handbook of Aluminium*, Volume 2 (Eds. G. E. Totten, D. S. MacKenzie), Marcel Dekker; New York, 2003. pp. 579-700
- [17] Veljić, D. et al., Heat Generation during Plunge Stage in Friction Stir Welding, *ThermalScience* (2013) doi: 10.2298/TSCI120301205V.
- [18] W. F. Noh. Cel: A time-dependent, two-space-dimensional, coupled eulerian-lagrangian code. *Methods in Computational Physics*, 3:117–179, 1964.
- [19] Vuppula Prasanna, Dr. A. Seshu Kumar, and Dr. P. Ramesh Babu, “Experimental Studies of Dissimilar Metals Welded Joint by F.S.W”, *Elsevier Materials Today: Proceedings* 18 (2019) 3276–3285.
- [20] Vuppula. Prasanna, Dr. P. Ramesh Babu, “The Effect of process Parameters on Microstructural and Mechanical Properties of Friction Stir Welded Age-Hardenable Aluminium Alloy’ *International Journal of Engineering and Advanced Technology (IJEAT)*, Volume-9, Issue-3, February-2020.
- [21] M. Hossfeld. Modelling friction stir welding: evolution of microstructure and weld geometry of aluminium

alloy 6061. Proceedings of the 39th MPA-Seminar, Stuttgart, 2013.

[22] M. Spittel and T. Spittel. Thermal expansion of light metal alloys. In H. Warlimont, editor, Part 2: Non-ferrous

Alloys - Light Metals, volume 2C2 of Landolt-Börnstein - Group VIII Advanced Materials and Technologies, pages 92–95. Springer, 2011.

[23] S. Guerdoux and L. Fourment. A 3d numerical simulation of different phases of friction stir welding. Modelling

and Simulation in Materials Science and Engineering, 17(7):075001, 2009.

[24] M. Vratnica, Microstructural properties and mechanical properties of highly hard aluminium alloys of Different grade of purity, doctoral thesis, Faculty of Technology –Metallurgy, Belgrade, Serbia, 2000

[25] Nandan. R, Roy. G.G, Lienert. T. J. and DebRoy T., Numerical modelling of 3D plastic flow and heat transfer

During friction stir welding of stainless steel, Science and Technology of Welding and Joining 11, 5, 52-537, 2006.